J|A|C|S
ARTICLES
Published on Web 01/10/2004

Scanning Tunneling Microscopy of Self-Assembled Phenylene Ethynylene Oligomers on Au(111) Substrates

Karsten Walzer,*[,†,||] Eike Marx,[‡] Neil C. Greenham,[‡] Robert J. Less,[§] Paul R. Raithby,[§] and Kurt Stokbro*[,†,⊥]

Contribution from Mikroelektronik Centret (MIC), Technical University of Denmark, Bldg. 345 East, DK-2800 Lyngby, Denmark, Cavendish Laboratory, Madingley Road, Cambridge, CB3 0HE, United Kingdom, and Department of Chemistry, University of Bath, Bath BA2 7AY, United Kingdom

Received June 19, 2003; E-mail: ks@atomistix.com; walzer@iapp.de

Abstract: In this paper, we report the self-assembly, electrical characterization, and surface modification of dithiolated phenylene-ethynylene oligomer monolayers on a Au(111) surface. The self-assembly was accomplished by thiol bonding the molecules from solution to a Au(111) surface. We have confirmed the formation of self-assembled monolayers by scanning tunneling microscopy (STM) and optical ellipsometry, and have studied the kinetics of film growth. We suggest that self-assembled phenylene ethynylene oligomers on Au(111) surfaces grow as thiols rather than as thiolates. Using low-temperature STM, we collected local current−voltage spectra showing negative differential resistance at 6 K.

Introduction

Phenylene ethynylene oligomers have attracted the interest of both physicists and chemists for their potential as the active element in future molecular electronic devices. Several approaches have been made to study their electronic properties, both by experimental and theoretical methods. Among these are conductance measurements in nanopores,[1,2] break-junctions,[3] and various scanning tunneling microscope (STM)[4,5] or conductive atomic force microscope (c-AFM)[6,7] setups, as well as theoretical studies using various approaches.[8−11]

One phenomenon of special interest in molecular electronics is the so-called negative differential resistance (NDR), which is characterized by a decreasing current at increasing voltage. NDR is the basic principle of several electronic components, as the resonant tunneling diode (RTD) and the Gunn diode. Especially, the RTD can be used as the basis of a simple memory device. Therefore, molecules possessing NDR properties may be utilized in molecular memory devices. NDR effects[1] as well as conductance switching[12] have already been observed for various oligomers. Our aim is to contribute to the knowledge about the NDR effect in such molecular films.

We have selected a dithiolated phenylene ethynylene trimer with a nitro side group on the central ring (see Scheme 1, molecule 1). Its monothiolated analogue has shown NDR in nanopore experiments[2] and in c-AFM.[7] We use dithiols instead of monothiols, because they allow a well-defined adsorption of molecules in two-terminal devices, such as gold nanogaps[13] or break junctions, provided such gaps can be produced with the correct width. In contrast to nanopore experiments, where typically thousands of molecules contribute to the measurement, the STM permits a very local conductivity measurement that only contacts very few molecules at a time.

Experimental Section

An Au(111) single crystal was used as substrate for STM measurements, prepared by sputter-anneal cycles in ultrahigh vacuum (UHV). For ellipsometry experiments, larger-area atomically flat films of Au(111) on mica were used. From our previous work we know that the two substrates have similar surface properties.

The thioacetate-protected molecule was synthesized as shown in Scheme 1 using a modification of the route reported by Tour et al.[2,14]

† Mikroelektronik Centret (MIC), Technical University of Denmark.
‡ Cavendish Laboratory, Madingley Road, Cambridge.
§ Department of Chemistry, University of Bath.
|| Present address: Institute of Applied Photophysics, Technical University of Dresden, D-01062 Dresden, Germany. Email: walzer@iapp.de.
⊥ Present address: Nanoscience Center, Copenhagen Univesity, Universitetsparken 5D, DK-2100 Copenhagen 0, Denmark.

(1) Chen, J.; Reed, M. A.; Rawlett, A. M.; Tour, J. M. *Science* **1999**, *286*, 1550.
(2) Chen, J.; Wang, W.; Reed, M. A.; Rawlett, A. M.; Price, D. W.; Tour, J. M. *Appl. Phys. Lett.* **2000**, *77*, 1224.
(3) Reichert, J.; Ochs, R.; Beckmann, D.; Weber, H. B.; Mayor, M.; von Löhneysen, H. *Phys. Rev. Lett.* **2002**, *88*, 176 804.
(4) Bumm, L. A.; Arnold, J. J.; Cygan, M. T.; Dunbar, T. D.; Burgin, T. P.; Jones, L., II.; Allara, D. L.; Tour, J. M.; Weiss, P. S. *Science* **1996**, *271*, 1705.
(5) Cygan, M. T.; Dunbar, T. D.; Arnold, J. J.; Bumm, L. A.; Shedlock, N. F.; Burgin, T. P.; Jones, L., II.; Allara, D. L.; Tour, J. M.; Weiss, P. S. *J. Am. Chem. Soc.* **1998**, *120*, 2721.
(6) Fan, F. F.; Yang, J.; Dirk, S. M.; Price, D. W., Jr.; Kosynkin, D. V.; Tour, J. M.; Bard, A. J. *J. Am. Chem. Soc.* **2001**, *123*, 2454.
(7) Fan, F. F.; Yang, J.; Cai, L.; Price, D. W., Jr.; Dirk, S. M.; Kosynkin, D. V.; Yao, Y.; Rawlett, A. M.; Tour, J. M.; Bard, A. J. *J. Am. Chem. Soc.* **2002**, *124*, 5550.
(8) Seminario, J. M.; Zacarias, A. G.; Tour, J. M. *J. Am. Chem. Soc.* **2000**, *122*, 3015.
(9) Karzazi, Y.; Cornil, J.; Brédas, J. L. *J. Am. Chem. Soc.* **2001**, *123*, 10 076.
(10) Kushmerick, J. G.; Holt, D. B.; Yang, J. C.; Naciri, J.; Moore, M. H.; Shashidhar, R. *Phys. Rev. Lett.* **2002**, *89*, 086 802.
(11) Taylor, J.; Brandbyge, M.; Stokbro, K. *Phys. Rev. Lett.* **2002**, *89*, 138 301.
(12) Donhauser, Z. J.; Mantooth, B. A.; Kelly, K. F.; Bumm, L. A.; Monell, J. D.; Stapleton, J. J.; Price, D. W., Jr.; Rawlett, A. M.; Allara, D. L.; Tour, J. M.; Weiss, P. S. *Science* **2001**, *292*, 2303.
(13) Sazio, P. J. A.; Berg, J.; See, P.; Ford, C. J. B.; Lundgren, P.; Greenham, N. C.; Ginger, D. S.; Bengtsson, S.; Chin, S. N. *Mater. Res. Soc. Symp. Proc.* **2001**, *B2.3.1.*, 679.

Scheme 1. Route of Chemical Synthesis and a Schematic of the Final Phenylene Ethynylene Oligomer Used in This Study in Its Protected (molecule 1′) and Unprotected Form (molecule 1).

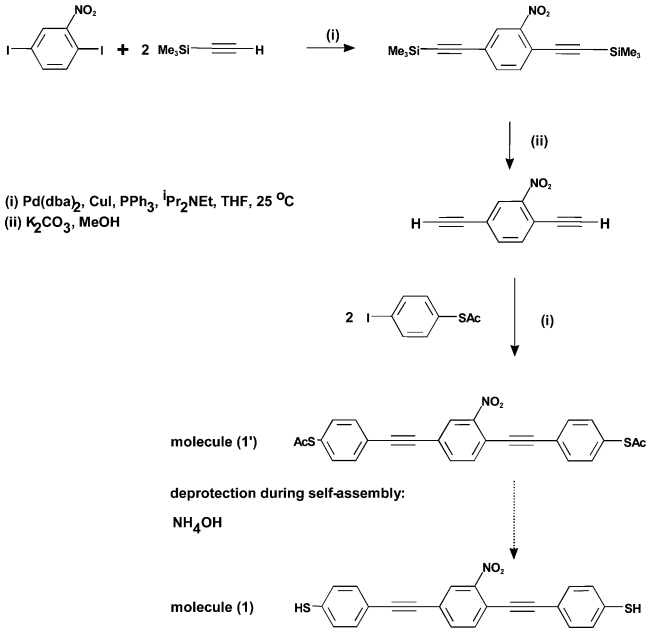

The details of the preparation are as follows: 1-nitro-2,5-diethynylbenzene (207 mg, 1.21 mmol) was added to a solution of 1-iodo-4-thioacetylbenzene (842 mg, 3.03 mmol), $Pd(dba)_2$ (50 mg), CuI (17 mg) and triphenylphosphine (70 mg) in 20 mL dry tetrahydrofuran under nitrogen, followed by diisopropylethylamine (0.84 mL, 4.8 mmol). The solution was stirred at room temperature for 16 h. The solution was filtered and the solvent removed. The residue was then dissolved in 20 mL dichloromethane and washed with 50 mL 0.1 M HCl followed by 50 mL saturated sodium bicarbonate solution and 50 mL brine, and then dried over magnesium sulfate. The crude product was purified by flash column chromatography (elutent 70:30 DCM/Hexane to give 546 mg (95%) yellow solid. MS (−FAB): 470.9 (M), 427.9, 341.9, 317.9, 303.0, 274.0, 258.0, 195.9, 180.9, 163.9, 155.0, 134.9, 123.0. IR (Nujol): 2211w (C≡C), 1693s (C═O), 1538w, 1527w, 1503w, 1346m, 1267w, 1093m, 1013w, 966w, 823m. ^{1}H NMR: 2.38 (6H, s, $COCH_3$), 7.36 (4H, d, *J* 7, ArH), 7.51 (2H, d, *J* 8, ArH), 7.55 (2H, d, *J* 8, ArH), 7.63 (2H, m, ArH), 8.16 (1H, m, ArH). ^{13}C NMR: 30.3 ($COCH_3$), 86.2, 88.3, 92.8, 98.0 (all C≡C), 117.9, 124.0, 127.7, 128.4, 129.0, 129.6, 130.5, 132.3, 132.5, 134.3, 134.8, 135.3 (all aromatic C). Analysis: $C_{27}H_{17}NO_4S_2$ calcd. C 66.22, H 3.63, N 2.97. Found C 66.9, H 4.10, N 2.41. The molecules were stored in this form protected from degradation by the acetyl end groups (see Scheme 1, molecule 1′).

The acetyl groups of molecule 1′ are removed during self-assembly by adding a small amount of ammonia to the solution. This deprotection activates the thiol end groups, which then react in situ with the Au(111) surface, forming self-assembled monolayers (SAMs). Our SAMs were grown at room temperature under nitrogen atmosphere from a 0.1 mM solution in tetrahydrofuran (THF) with ammonia added. As we will report in the next section, growth times of 21 h were found to be the optimum for self-assembly of the molecules used. After self-assembly, the films were rinsed with pure THF and dried under a stream of nitrogen. For STM measurements, the films were immediately inserted into UHV.

All STM measurements were made in UHV at a base pressure below 2×10^{-10} mbar. We used a low-temperature STM as described elsewhere[15] with electrochemically dc-etched tungsten tips. Immediately before insertion into UHV, the tips were further cleaned by a 1 min etch in 5% hydrofluoric acid to remove organic contaminants. STM measurements were done both at 300 and 6 K.

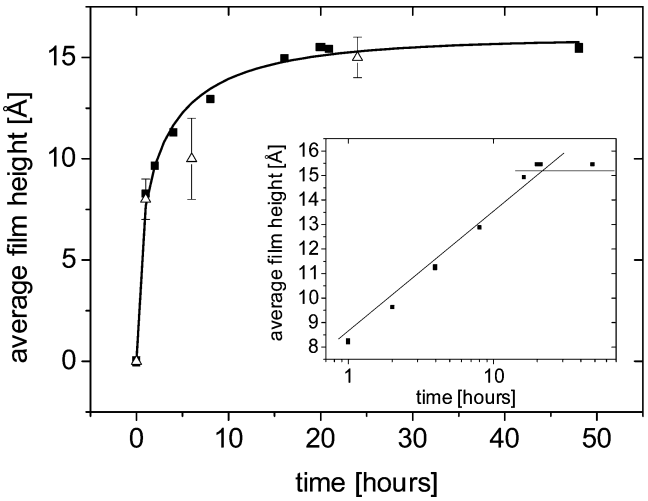

Figure 1. Time development of SAM growth as measured by ellipsometry (squares). The STM measurement of the film thickness is also shown (open triangles). The fitted curve shows the time dependence of growth as calculated from the ellipsometry data by eq 3. Inset: Growth and saturation can clearly be distinguished from each other. (The lines are only guides for the eye).

Ellipsometry data were collected under ambient conditions using a J. A. Woollam M-2000 variable angle spectroscopic ellipsometer at angles of 45°, 50°, 55°, 60°, and 65° over the wavelength range 300−500 nm. Until measurement, the samples were stored under nitrogen atmosphere to avoid oxidation of the molecules.

Results and Discussion

(a) Film Thickness and Formation. Prior to measurement of the electronic properties of the molecular films, the monolayer growth was studied. We wish to determine the angle between the assembled molecules and the substrate, to investigate whether the molecules assemble in an upright standing configuration, or whether both sulfur atoms bind to the surface, causing the molecules to lie flat. Ellipsometry was used to study film growth, and STM measurements were used to confirm the final film thickness.

In general, it is rather difficult to determine the thickness of ultrathin films such as SAMs using ellipsometry, unless the optical constants are known independently. Because the molecules studied here are conjugated, their refractive index is likely to be significantly larger than the values typically assumed for aliphatic SAMs. We have therefore attempted to determine both the thickness and optical constants of the SAMs from the ellipsometric data. To reduce correlations between the fitting parameters in our optical model, we constrain the optical constants of the SAM to reproduce the shape of the absorption spectrum measured in solution. Full details of the modeling procedure are described elsewhere.[16,17]

Figure 1 shows the ellipsometrically determined film thickness as a function of assembly time, defined by the average thickness of the film. Although it is difficult rigorously to model

(14) Tour, J. M.; Jones II, L.; Pearson, D. L.; Lamba, J. J. S.; Burgin, T. P.; Whitesides, G. M.; Allara, D. L.; Parikh, A. N.; Atre, S. V. *J. Am. Chem. Soc.* **1995**, *117*, 9529.

(15) Made by VTS−Createc, Erligheim, Germany, after a design of Meyer, G.; see: Meyer, G. *Rev. Sci. Instr.* **1996**, *67*, 2960.

(16) Marx, E.; Ginger, D. S.; Walzer, K.; Stokbro, K.; Greenham, N. C. *Nano Lett.* **2002**, *2*, 911−914.

(17) Marx, E.; Walzer, K.; Less, R. J.; Raithby, P. R.; Stokbro, K.; Greenham, N. C., submitted to Org. Electronics.

the optical properties of partially assembled films, the film thickness determined gives a good indication of the average coverage of molecules on the surface. It can be seen that the initial growth is fast, followed by saturation after about 21 h to a thickness of 15.5 Å, corresponding to monolayer formation. Subsequent scanning tunneling spectroscopy experiments were therefore performed after assembly times of at least 21 h.

The shape of Figure 1 suggests a Langmuir-type growth. Such a Langmuir model considers in its simplest case an irreversible statistical adsorption, which can be described as

$$\frac{d\theta}{dt} \propto 1 - \theta \tag{1}$$

where θ is the fractional surface coverage. This behavior leads directly to the time-dependent coverage

$$\theta(t) = 1 - e^{-k_L t} \tag{2}$$

The parameter k_L is the Langmuir adsorption constant for a given solution concentration (in our case $c = 0.1$ mM). Because we were not satisfied with the fitting of this simple sticking model to our data, we chose a somewhat more sophisticated Langmuir model, which also considers the diffusion limitation induced by the film growth[18,19]

$$\theta(t) = 1 - e^{-k_{LD} t^{1/2}} \tag{3}$$

The fitted curve shown in Figure 1 is calculated from the ellipsometry data using this equation, with a diffusion-limited Langmuir rate constant of $k_{LD} = 0.011$ s$^{-1/2}$. This is significantly smaller than the corresponding value for hexadecanethiol,[19] (0.08 s$^{-1/2}$ at the same concentration), corresponding to a film formation speed that is nearly 2 orders of magnitude slower than that for alkanethiols. This can be explained by steric hindrance between the stiff molecules during the growth. Fitting the experimental data to the form of eq 3 leads to a calculated final film thickness of 15.9 Å.

The film thickness obtained with ellipsometry is an average thickness in an area of size ~1 μm^2. To confirm that this average thickness agrees with the local film thickness, we performed SAM thickness measurements by STM. These measurements were performed by selectively removing molecules from a particular area using a low tunneling resistance, and measuring the height difference of the freshly made hole in the SAM. To measure this height, the STM was operated in constant current mode (see the Supporting Information for details).

Usually, SAMs of molecules similar to the ones used in this study are imaged by scanning at GΩ tunnel resistances (tunnel resistance = bias voltage/setpoint current). This allows imaging of the surface of the molecular film without significant changes of the molecular order at least on the time-scale of tens of minutes. After imaging under these conditions, we switched to significantly lower tunnel resistances (a few MΩ). This causes the tip to approach the metallic substrate, removing the molecular film on the metal surface. Thus, a window is scratched into the film, whose height can be measured afterward by cross-section measurements or by use of a histogram. We have chosen the latter to reduce the effect of noise.

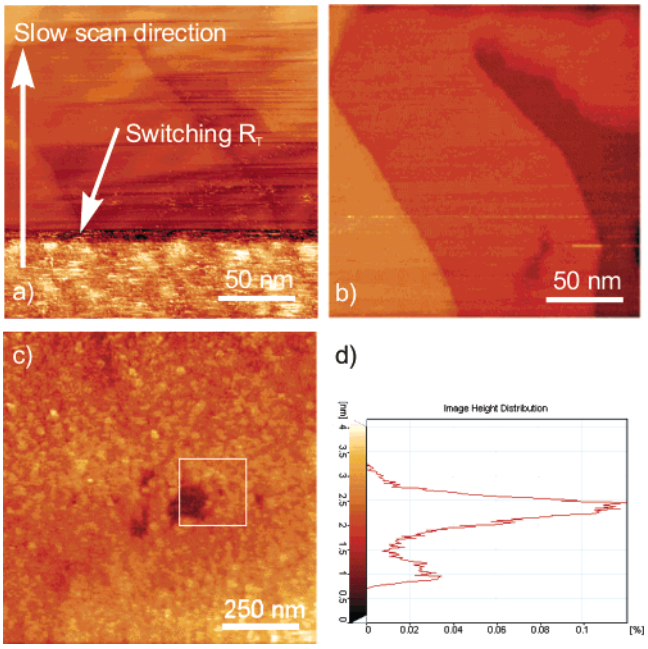

Figure 2. (a) Switching of the tunnel resistance from 3 GΩ to 25 MΩ. Height scale: 4 nm. Whereas in the lower part of the image the SAM is shown at high tunnel resistance, after switching to low resistance this film is removed by "scratching" with the STM tip, and the underlying Au(111) substrate can be observed. The stripes in the image result from molecules moving under the influence of the tip. (b) Underlying Au(111) substrate with monolayer steps which become visible during removal of the SAM. (c) Zoom-out image at high tunnel resistance, showing a dark window where the molecular film is removed. (d) Histogram of the height distribution measured inside the white square shown in (c), revealing a film height of (15 ± 1) Å. $T = 300$ K.

Figure 2 shows the different phases of such an experiment. In our case, the window was scratched at a low-tunnel-resistance regime of 0.11 V and 4 nA, whereas the larger image shown in Figure 2c was measured at high tunnel resistance again, with a bias of 2.5 V and a feedback current of 0.8 nA. The histogram shown in Figure 2d reveals two peaks resulting from substrate and adsorbate. The difference of (15 ± 1) Å between the maxima corresponds to the film height, in good agreement with the thickness determined by ellipsometry.

A similar time development as we just have seen by ellipsometry (Figure 1) can also be observed by STM: The STM data given above refer to films grown for 24 h. In case of shorter growth times we found in our STM images average film thicknesses of (8 ± 1) Å after 1 h growth, and (10 ± 2) Å [more noisy] after 6 h. (The average height was determined by measuring height distribution histograms of several windows made in the same manner.) Thus, our STM data of the local thickness are consistent with the results of the ellipsometric measurements of the average film thickness, see the open triangles in Figure 1.

(b) Surface Bonding. The measured film height of approximately 15.5 Å can be compared with calculated geometry data of the molecule. We have used the semiempirical PM3 method as implemented in the Gaussian 98 software package.[20] The calculated length (the sulfur−sulfur distance) of the individual unprotected molecule is 19.9 Å, and we estimate a total molecular length of approximately 22 Å when it is bonded to the Au surface. Thus, the measured film thickness corresponds roughly to 3/4 of the molecular length, implying that the

(18) Dannenberger, O.; Buck, M.; Grunze, M. *J. Phys. Chem. B* **1999**, *103*, 2202.
(19) Peterlinz, K. A.; Georgiadis, R. *Langmuir* **1996**, *12*, 4731.

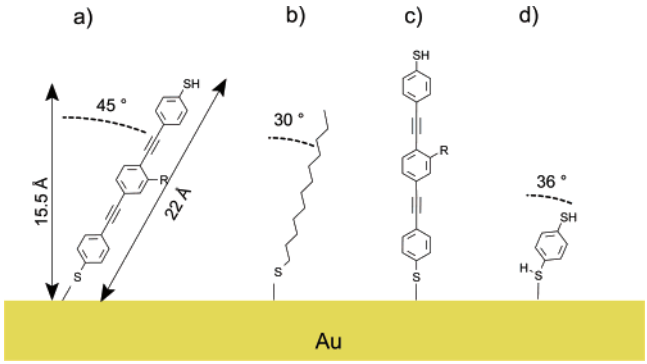

Figure 3. (a) The tilt angle of the oligo phenylene ethynylene monolayer, as suggested from the measured height of the SAMs, and the theoretical length of the molecule. (b) The average experimentally observed tilt angle of alkanethiol SAMs. (c) Theoretical model of the adsorption geometry of thiolate bonded oligo phenylene ethynylenes. (d) Theoretical adsorption geometry of phenyl dithiol which is thiol bonded to gold (the SH bond is intact).

molecules in the layer are tilted by approximately 45° relative to the surface normal (Figure 3a).

Similar data have been published recently for experiments with SAMs of a closely related molecule: Dunbar et al.[21] determined the molecular tilt of another oligo phenylene ethynylene on Au(111) by infrared spectroscopy. They found a tilt angle of 37 ± 15°, which is consistent with our value. The end group bonding to the gold was the same for both experiments, whereas the chain length and the substitution of the molecules were different.

We would like to relate the tilt angle with a specific adsorption geometry of the molecule. For this purpose, it is instructive to compare the results with experimental and theoretical work on the adsorption of alkanethiols to gold. The adsorption of alkanethiols to gold is an intensively studied system, and there is now general consensus that the molecular axis of alkanethiols is tilted by ~30° with respect to the gold substrate plane.[22] Although numerous experimental and theoretical works have tried to relate this tilt angle with a specific adsorption geometry, the adsorption geometry is still an open question. Here, we would like to note that the tilt angle of alkanethiols is a result from both the Au−S−C bond angle, θ_{Au-S-C}, and the internal S−C−C bond angle, $\theta_{S-C-C} = 109°$, giving rise to a tilt angle of $\theta_{tilt} = \theta_{Au-S-C} \pm (180°-109°)/2$. (We assume that θ_{Au-S-C} and θ_{S-C-C} lie in the same plane. If this would be not the case, the total molecular tilt would be smaller, and the calculated film thickness would be larger than we observe.)

If the rod like oligo(phenylene-ethynylene) (OPE) system had the same adsorption geometry as the alkanethiols, then θ_{Au-S-C} would be the same. However, the observed tilt angle θ_{tilt} would be different, because in this case $\theta_{S-C-C} = 180°$. The fact that we observe a tilt angle similar to the alkanethiol systems indicates that the OPEs are bonded differently. This might not be that surprising because for OPE the S atom is attached to a π-conjugated molecule and therefore forms a double bond with the neighboring *unsaturated* C atom, whereas for alkanethiols the S atom forms a single bond with the neighboring *saturated* C atom. Instead, we would like to relate our results for OPE to our previous theoretical studies of phenyl-dithiol (PDT) adsorbed on gold surfaces.[23] Both OPEs and PDT are π-conjugated molecules and the S atom forms a double bond with the neighboring *unsaturated* C atom. Thus, they likely have similar adsorption geometries. In the case where PDT is adsorbed in the 3-fold hollow site, the tilt angle is 0°. However, if the strong SH bond is not cleaved, and the molecule forms a thiol bond with gold, our calculation predicts a tilt angle of 36° for phenyl-dithiol adsorbed at the on top site (Figure 3d). Because this angle is rather similar to the experimentally observed tilt angle of OPE, we speculate that the strong SH bond is not cleaved for the OPE molecule, which would give rise to an adsorption in an on-top position with a tilt angle ~36°. Other theoretical and experimental work supports the idea that such thiol-bonded molecules may exist on the surface: Theoretical calculations by Andreoni et al. indicate that the adsorption energy of thiol and thiolate bonds differ by less than 0.1 eV,[24] suggesting that both bonds may be realized dependent on the growth conditions of the SAM. STM measurements of PDT show the existence of two different adsorption geometries, where in the one geometry, PDT is adsorbed on the on top site.[25] Because thiol-bonded molecules are adsorbed at the on top site, whereas thiolate-bonded molecules are adsorbed in higher coordinated sites, like the hollow or bridge site[24,26] this suggests further that thiol-bonded molecules may exist on the surface.

During the STM experiments we also observed sample changes after long scan times. Figure 4, parts a and b, shows the same surface area before and after 14 h of scanning at a feedback of +2 V, 150 pA. Scanning under these conditions changes the surface slowly, i.e., in the range of a few hours, but subsequent scans appear to be stable. After many hours of scanning a formation of small domains or clusters is observed, as can be seen in Figure 4b. These molecular domains show a height variation of around 1.0 nm which leads us to the conclusion that the structure of the SAM in the different areas has been changed. It should be noted that no molecular resolution could be found in our STM images, neither at freshly deposited films nor after the surface changes described above. This result is consistent with the fact that also in the literature other STM studies did not report ordered structures of oligo-(phenylene−ethynylenes) *with* side groups, whereas oligo-(phenylene−ethynylenes) *without* side chain, as they were studied by Dhirani et al.,[27] form well-ordered molecular domains. Therefore, we conclude that the steric hindering caused

(20) Frisch, M. J.; Trucks, G. W.; Schlegel, H. B.; Scuseria, G. E.; Robb, M. A.; Cheeseman, J. R.; Zakrzewski, V. G.; Montgomery, J. A., Jr.; Stratmann, R. E.; Burant, J. C.; Dapprich, S.; Millam, J. M.; Daniels, A. D.; Kudin, K. N.; Strain, M. C.; Farkas, O.; Tomasi, J.; Barone, V.; Cossi, M.; Cammi, R.; Mennucci, B.; Pomelli, C.; Adamo, C.; Clifford, S.; Ochterski, J.; Petersson, G. A.; Ayala, P. Y.; Cui, Q.; Morokuma, K.; Malick, D. K.; Rabuck, A. D.; Raghavachari, K.; Foresman, J. B.; Cioslowski, J.; Ortiz, J. V.; Stefanov, B. B.; Liu, G.; Liashenko, A.; Piskorz, P.; Komaromi, I.; Gomperts, R.; Martin, R. L.; Fox, D. J.; Keith, T.; Al-Laham, M. A.; Peng, C. Y.; Nanayakkara, A.; Gonzalez, C.; Challacombe, M.; Gill, P. M. W.; Johnson, B. G.; Chen, W.; Wong, M. W.; Andres, J. L.; Head-Gordon, M.; Replogle, E. S.; Pople, J. A. *Gaussian 98*, revision A.7; Gaussian, Inc.: Pittsburgh, PA, 1998.
(21) Dunbar, T. D.; Cygan, M. T.; Bumm, L. A.; McCarty, G. S.; Burgin, T. P.; Reinerth, W. A.; Jones, L., II.; Jackiw, J. J.; Tour, J. M.; Weiss, P. S.; Allara, D. L. *J. Phys. Chem. B* **2000**, *104*, 4880.
(22) Schreiber, F. *Prog. Surf. Sci.* **2000**, *65*, 151.
(23) Stokbro, K.; Taylor, J.; Brandbyge, M.; Mozos, J.-L.; Ordejon, P. *Comput. Mater. Sci.* **2003**, *27*, 151.
(24) Andreoni, W.; Curioni, A.; Gronbeck, H. *Int. J. Quantum Chem.* **2000**, *80*, 598.
(25) Li-Jun Wan, H. N.; Terashima, M.; Osawa, M. *J. Phys. Chem. B* **2000**, *104*, 3563.
(26) Vargas, M. C.; Giannozzi, P.; Selloni, A.; Scoles, G. *J. Phys. Chem. B* **2001**, 105.
(27) Dhirani, A.; Zehner, R. W.; Hsung, R. P.; Guyot-Sionnest, P.; Sita, L. R. *J. Am. Chem. Soc.* **1996**, *118*, 3319.

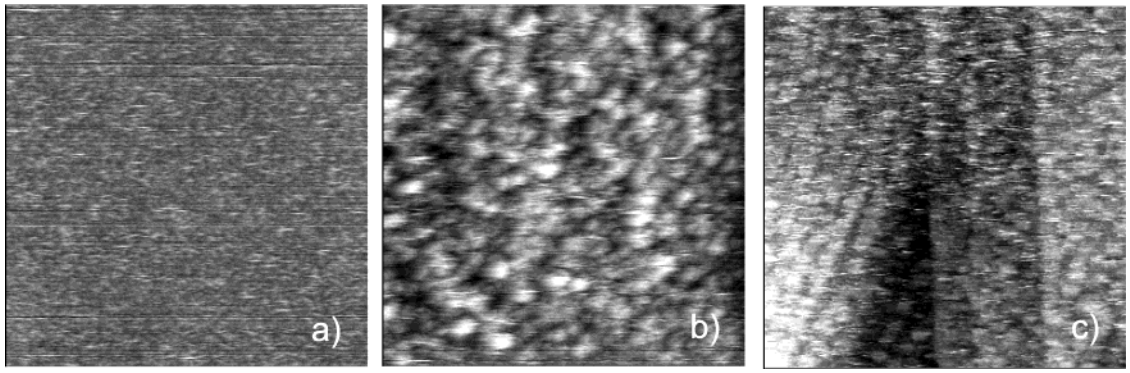

Figure 4. (a) Overview image at the beginning of a scan experiment and (b) after 14 h: Whereas the original film is mainly homogeneous, after 14 h of scanning the surface has changed significantly. These changes appear gradually. Both images: (450 × 450) nm^2, $U = 2$ V, $I = 150$ pA, $T = 300$ K, identical gray scale. The height scale is 10 Å. No ordered molecular structure could be resolved by STM, even at higher resolution. (c) After annealing for 2 h at 85 °C in UHV a pattern of ordered small domains of similar size as after the scan experiment can be found. The sharp lines in the image are caused by steps in the underlying gold substrate.

by the NO_2 side chain anticipates the formation of a well-ordered 2d crystal on the Au surface. The lower packing density within the films of molecules having side chains leads further to a reduced cooperative stabilization and thus to a lower resolution of the STM images.

Changes in the molecular order can also be created by thermal annealing of the samples under UHV conditions, as we could show by annealing at 85 °C for 2 h. An image of the resulting pattern is presented in Figure 4c. The domains are arranged along the monatomic steps of the underlying gold substrate. Typically, these structures are 5 to 10 nm in diameter, and below 1 nm in height. This corresponds to a rearrangement of the molecular monolayer. However, the internal structure of the bright domains is unknown, and could not be resolved by STM. We conclude that the growth of such domains under the influence of an activation energy (coming from an electric field, a tunneling current or from thermal activation) is energetically favorable over the homogeneous molecular order. This, together with the proposed structure of the virgin film, indicates that the strong SH bond may only be cleaved by thermal treatment or under influence of the STM current/electric field, and that the bright domains in Figure 4, parts b and c, are areas where the molecules form thiolate bonds.

(c) Current−Voltage Spectroscopy. Local I/V spectra were collected in the low-temperature STM at 6 K to study the conductance properties of the SAMs. The sweeps were done at a feedback position of +940 mV and 280 pA, where we measured a very stable tunnel contact. The voltage was swept from −3 to +3 V with the feedback loop switched off, within a time of 60 s per sweep (Figure 5). Before and after collecting the spectroscopy data, the surface was checked for possible changes by STM imaging. Only I/V scans without any surface changes were evaluated. It should be noted that surface changes within this bias window were very rare. When a surface change was observed, those STS data were discarded, and a fresh surface area was taken for further measurements. As a control experiment, the instrument was checked by collecting I/V curves on bare Au(111). These curves showed the smooth behavior as known for gold, with no evidence of artificial peaks. Therefore, we conclude that the peaks observed arise from the interplay of the adsorbed molecular film with the metal electrodes and the applied voltage.

We found strong negative differential resistance (NDR) peaks in our SAMs. NDR means that for a certain bias window an

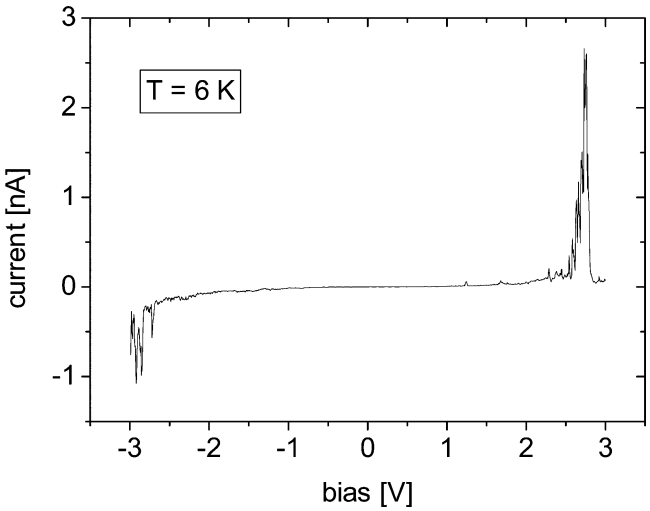

Figure 5. Typical individual I/V curve of molecule 1 on Au(111) showing negative differential resistance. In this case, a peak-to-valley ratio of 60 is observed around +2.8 V. The curve was measured by slowly sweeping the sample bias from −3 to +3 V (sweep time: 60 s).

increase in the bias leads to a decrease in the measured current. Mostly, one NDR feature was present in an I/V curve (in forward and reverse scan), however, in some cases also two or more peaks were observed. Although we tried to collect spectra at the same position, a lateral drift of a few angstroms between individual scans cannot be ruled out because the molecules were standing and bound to the substrate only at one end. There was considerable variation in the position of the NDR features between different scans, and in their strength (measured by the peak-to-valley ratio). The statistics of the position and strengths of the NDR features are represented in Figure 6. The most common NDR feature was found at around +2.8 V, and these features typically had also the highest peak-to-valley ratios (up to 100:1). Other frequent NDR peak positions were around −2.8, −2.4, and +2.2 V, but there were smaller NDR features over a wide range of energies. The observed NDR events were not bias-symmetric, i.e., NDR in one polarity does not necessarily require another event under opposite polarity.

Previous work by Fan and co-workers[7] for the monothiolated analogue of our molecule showed a weak peak (with a peak-to-valley ratio below 2:1) at + 2.6 V and a strong peak (peak-to-valley ratio above 10:1) at −2.8 V. Our measurements show peaks at similar positions. Another recent study made by Rawlett

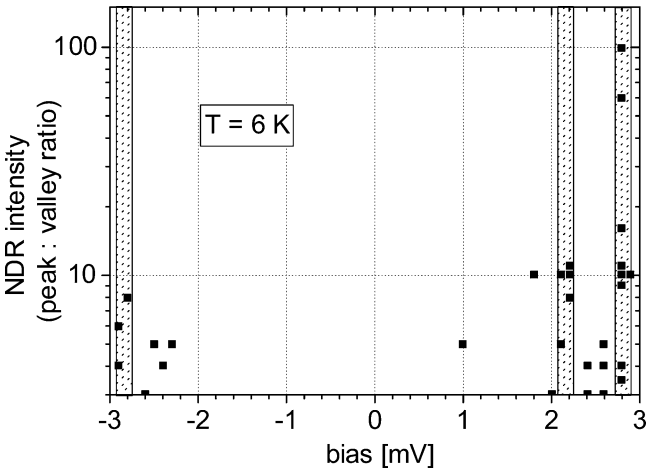

Figure 6. Statistics of the NDR event number and NDR intensity versus peak voltage. The peaks are taken from 38 voltage sweeps as described in Figure 5 taken subsequently at adjacent positions on the same sample. The most frequent and strongest NDR signals were found around −2.8, +2.2, and +2.8 V, with the +2.8V peak being the one both with most NDR events and highest NDR ratios. Peaks with a peak-to-valley ratio below 3:1 were disregarded for this graph.

and co-workers[28] using a conductive AFM tip found an NDR effect for isolated entities of the same molecule when positioned in a matrix of alkanethiols. The peak positions were located at lower voltages than our typical peaks, somewhat above 1 V. Some of these experiments also showed more complex switching effects, which we do not observe. The differences can be ascribed to the very different experimental conditions: unlike Rawlett's data, our data were collected at low temperatures, in UHV, and on a monolayer of conjugated molecules rather than on molecules isolated in a matrix.

A number of theoretical attempts have been made to explain the origin of NDR effects in conjugated oligomers.[8,29,30] Calculations by Cornil and co-workers[29] and by Stokbro and co-workers[30] have shown the importance of rotations of the central phenyl ring in explaining the NDR. When the middle ring is rotated the π conjugation of the molecule is broken, and the middle ring acts as a tunnel barrier between the two outer phenyl rings. The electronic states of the outer rings will now be isolated, and a high current only arises when two states align. Such alignment may arise at specific electric fields, corresponding to specific biases where there is a high resonant current. Geometries with the middle ring rotated may arise for oligo phenylene ethynylenes with nitro side groups, because the nitro group can stabilize such structures due to hydrogen bonding with neighboring molecules.[31] The different local environments of molecules within the SAM can thus explain the variation in position and shape of the NDR at different positions on the SAM surface.

(28) Rawlett, A. M.; Hopson, T. J.; Nagahara, L. A.; Tsui, R. K.; Ramachandran, G. K.; Lindsay, S. M. *Appl. Phys. Lett.* **2002**, *81*, 3043.
(29) Cornil, J.; Karzazi, Y.; Brédas, J. L. *J. Am. Chem. Soc.* **2002**, *124*, 3516.
(30) Stokbro, K.; Taylor, J.; Brandbyge, M.; Ordejon, P. *Ann. N. Y. Acad. Sci.*, in press.

Conclusion

Using optical ellipsometry, scanning tunneling microscopy, and scanning tunneling spectroscopy, we have investigated the growth behavior of a phenylene ethynylene oligomer on Au(111) surfaces. We found that the molecules form a monolayer with the molecular axis tilted at an angle of approximately 45° to the substrate normal. The monolayer growth saturated after approximately 21 h, which is nearly 2 orders of magnitude slower than the growth of alkanethiol SAMs. Immediately after self-assembly, the films are homogeneous, whereas after energy input (by STM scanning or annealing) a rearrangement of the molecules was found. Our results suggest that the molecules are initially deposited in the thiol form, with SH groups present at the surface. At low temperatures, the films show negative differential resistance at voltages of typically +2.8 V. We suggest that this NDR arises when the middle ring of the molecule is rotated.

Acknowledgment. The authors would like to thank P. J. Wilson for checking the purity of the organic material. The work was funded by the European Commission within the 5th framework IST program under Contract No. IST-1999-10323, "SANEME", by the Danish Technical Research Council (STVF), and the Engineering and Physical Sciences Research Council (EPSRC), UK. E.M. was partly funded by the DAAD (Deutscher Akademischer Austauschdienst).

Supporting Information Available: Some assumptions and details for the modeling can be found as Supporting Information. Further, the issue of reproducibility of the I/V spectra is discussed there. The material is available free of charge via the Internet at http://pubs.acs.org.

JA036771V

(31) Taylor, J.; Brandbyge, M.; Stokbro, K. *Phys. Rev. B* **2003**, *68*, 121101(R).